

Ultrahigh-Power Semiconductor Diode Laser Arrays

PETER S. CROSS, GARY L. HARNAGEL, WILLIAM STREIFER,
DONALD R. SCIFRES, DAVID F. WELCH

The power available from transistor-sized semiconductor diode lasers has increased rapidly in recent years, more than doubling every year. Continuous outputs of several watts and pulsed powers in the kilowatt range with 50 percent overall efficiency are now possible with these compact devices. These developments may signal the start of a technological advancement in optics comparable to the solid-state revolution in electronics 20 years ago.

SEMICONDUCTOR DIODE LASERS ARE SOLID-STATE DEVICES that directly and efficiently convert electrical into optical energy. In many respects, diode lasers represent a technological advance from the more common gas lasers (such as the familiar red, helium-neon lasers) that is similar to the transistor's advance over the vacuum tube. These lasers are already firmly established in a number of applications requiring light sources of small size and high reliability, including long-haul telecommunications, compact audio disk players, and computer memories. For these uses, relatively low-power beams of a few milliwatts are adequate. There are, however, many other applications that require substantially higher output power.

In recent years, through the use of multi-emitter laser arrays, great improvements have been made in the power and efficiency achievable at room temperature from these small, robust sources of optical energy. For example, continuous wave (cw) power in excess of 5 W has been demonstrated with a monolithic array of 100 emitters (1), which is greater than 1000 times more powerful than the lasers in compact disk players. Further, more than 100 W with 50% power conversion efficiency was obtained in 150- μ sec pulses from a monolithic linear array of 1000 lasing emitters (2), and such linear arrays have been stacked in a dense, two-dimensional configuration

to achieve a quasi-cw power density in excess of 3 kW/cm² at a wavelength of about 810 nm (3).

These advances have made possible applications that were unattainable only a few years ago, including efficient, all-solid-state lasers in the visible and near infrared; fiber-optic power transmission for industrial and medical uses; laser-initiated pyrotechnic ignition; and satellite optical communications.

Diode Laser Array Design

The highest power diode lasers have been achieved with the use of aluminum gallium arsenide (AlGaAs) ternary crystal alloys. A schematic diagram of a typical multi-emitter diode laser array is shown in Fig. 1 (4). The device consists essentially of a series of very thin crystalline layers (less than 10 μ m in total thickness) of AlGaAs grown epitaxially on a GaAs substrate. The thickness of the complete structure is approximately 100 μ m. Of this thickness, only three portions (less than 5 μ m thick in total) are of importance in the lasing process. The central region is the quantum well (QW) active layer, which is about 50 nm thick. When a small voltage (slightly greater than 1.5 V) is applied to the diode, electric current flows and carriers (electrons and holes) are injected into the active region. Upon recombining, the carriers generate light.

The active region of the laser consists of one or more very thin layers (typically less than 10 nm thick). Because these layer thicknesses are comparable to the quantum mechanical wavelength of the carriers, the properties of the material change. Specifically, the allowed energy states become discrete or quantized (5). This energy level quantization enhances the radiative recombination of carriers, which improves performance of diode lasers.

The optical emission wavelength is determined by the energy band gap of the alloy material in the active region. For the AlGaAs system, the nominal range of achievable wavelengths is between about 680 and 860 nm, in the near-infrared portion of the spectrum. Since the energy gap varies with alloy composition, the emission wavelength is coarsely determined by choosing the appropriate mole fraction of aluminum in the active region wells.

The maximum power available from a diode laser is generally limited (because of surface damage) by the emission area of the crystal facet. To achieve stable, high-power laser operation, it does not suffice simply to widen the area because uncontrolled filamentary oscillation can occur and lead to destruction of the device. Rather, it is necessary to divide the active region into a multi-emitter array (Fig. 1). The active aperture is thus broken into several separate emitters by means of proton bombardment, which creates insulating regions that channel current to 3- to 8- μ m-wide stripes typically

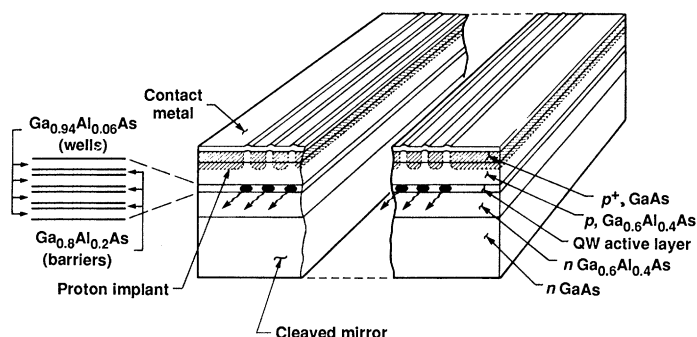


Fig. 1. Schematic diagram of a multi-emitter AlGaAs laser array using a quantum well (QW) active region for high power and efficiency.

The authors are with Spectra Diode Laboratories, San Jose, CA 95134.

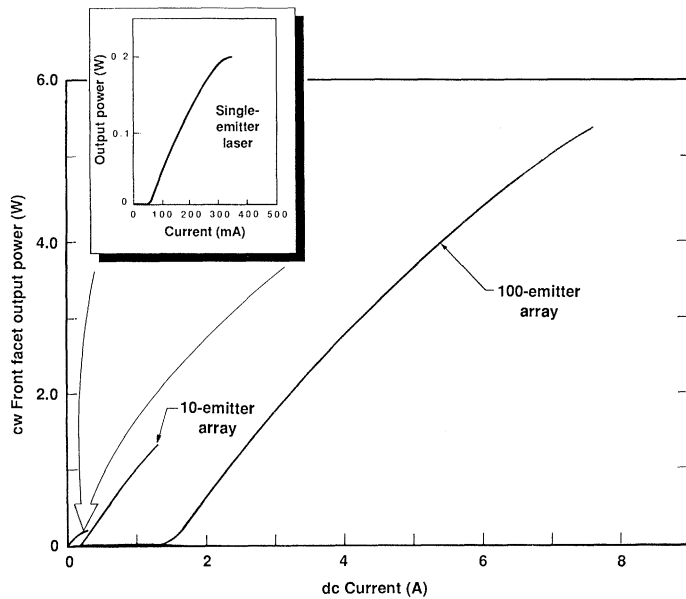


Fig. 2. Comparison of the light-versus-current characteristics of three semiconductor laser devices: a single-emitter laser, a 10-emitter array, and a 100-emitter array. These data are the absolute maximum powers for each device, beyond which they fail rapidly.

placed on 10- μm centers. With this multi-emitter array approach, laser emission is largely confined to the regions between the insulating stripes, thereby suppressing spurious filamentary oscillation.

Multi-Emitter Array Fabrication

The fabrication process for multi-emitter laser arrays begins with the epitaxial growth of the desired crystalline layers on an *n*-type GaAs substrate by means of the metal-organic chemical vapor deposition (MOCVD) method. The GaAs substrate is placed on a

platform heated to 800°C inside a quartz reaction vessel, and then reactive gases (typically metal-organic compounds such as trimethylaluminum and trimethylgallium, and other gases such as arsine) are sequentially admitted to the vessel under computer control. The composition and thickness of the deposited layers are determined by adjusting the gas flow rates, reaction times, and substrate temperature. The MOCVD growth technique has proved ideal for producing the uniform thin layers necessary for achieving high-efficiency, high-power diode laser arrays (6).

After completion of the layer growth, the wafer is processed with a planar technology similar to that used for silicon integrated circuitry. The active stripe emitters are protected by a pattern in a photosensitive material, and the wafer undergoes proton bombardment to destroy conductivity between the stripes. Next, the wafer is metallized to provide electrical contacts and is then scribed and cleaved into bars about 250 μm wide by 1 cm long, each containing 10 to 20 multistripe arrays. The parallel cleaved facets are subsequently coated with a high-reflectivity mirror coating on the rear facet and a transparent passivation or partial antireflection layer on the output facet. Optical feedback is thus provided by a mirror surface that is an integral part of the laser chip itself and is therefore automatically aligned with the gain medium, in contrast to the external mirrors of a gas or solid-state laser.

The bars are next separated into individual arrays before being soldered to a heat sink or submount. Each chip is about 500 μm by 250 μm by 100 μm and may contain as many as 40 laser emitters. Wire bonds are attached after the bars are soldered, and parametric and burn-in (extended operation at elevated temperature) testing are performed. Devices passing burn-in are then assembled into a hermetically sealed package.

Continuous Wave Array Performance Characteristics

The performance of diode lasers is often presented in terms of the light-versus-current characteristics, as shown for a number of devices in Fig. 2. Typically, as the drive current is increased from zero, the light output rises slowly with low-quantum efficiency. This is the

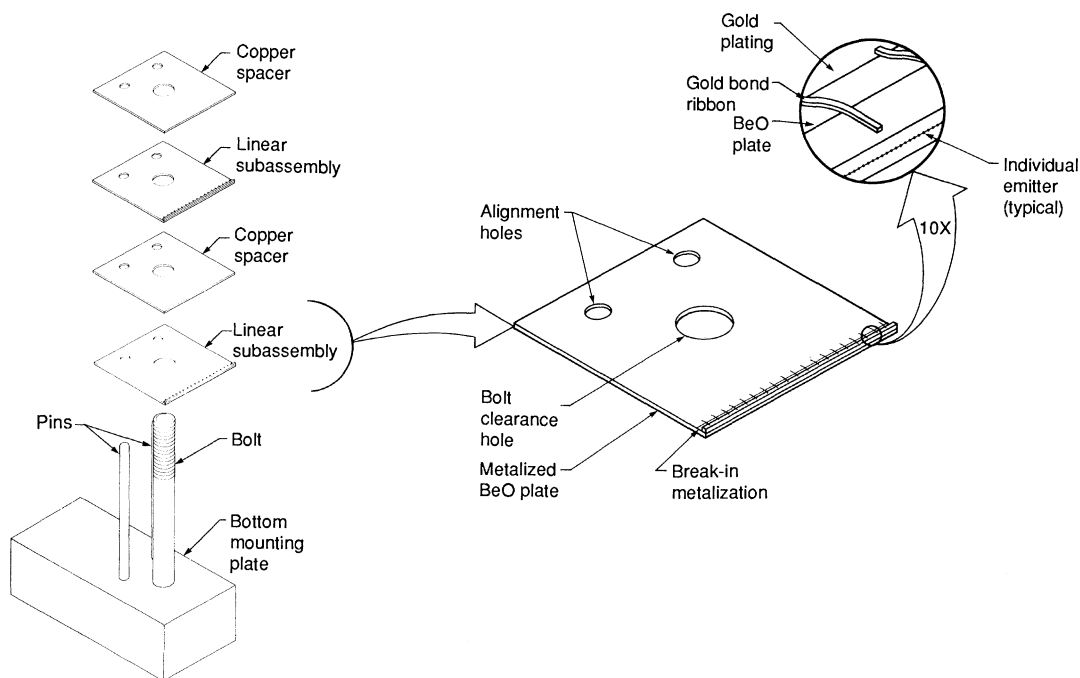


Fig. 3. Exploded schematic diagram of a high-density, two-dimensional array of diode lasers. As many as 30,000 laser emitters can be stacked within 1 cm^2 to produce more than 3 kW of output power in long pulses.

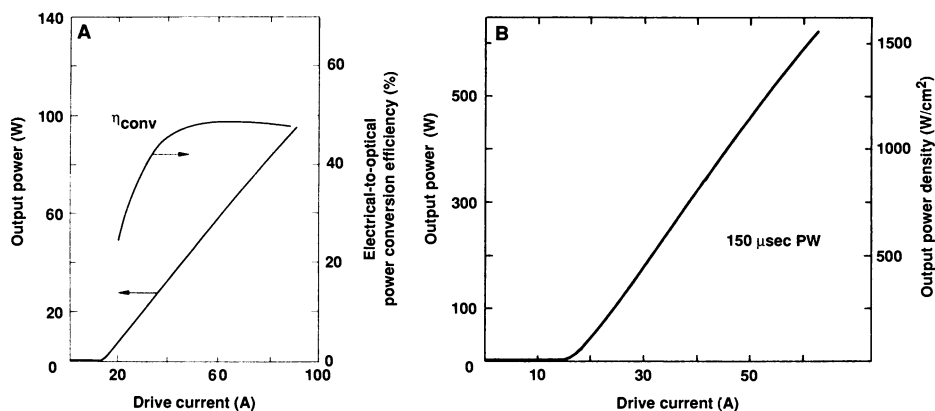


Fig. 4. (A) Output power and power conversion efficiency (η_{conv}) versus drive current for a high-quality linear array of 1000 emitters. (B) The light-versus-current characteristics of a high-density, two-dimensional array. PW, pulse width.

domain in which spontaneous emission operates in light-emitting diodes (LEDs). Above a certain threshold current, the optical gain in the active region is sufficient to initiate laser oscillation, and the output rises steeply. Above threshold, the incremental ratio of photons emitted to carriers injected (the differential quantum efficiency) can exceed 80%.

The highest reported continuous wave (cw) power achieved from a single emitter diode laser is in the range of 200 to 250 mW (7). Above this power, the optical intensity in the device becomes so high that, even in the best devices, the mirror facets melt in a catastrophic thermal runaway process (8). By spreading out the power through the use of a multi-emitter array, the power at which catastrophic failure occurs can be increased substantially. In a 10-emitter array, this power is increased to about 1.5 W (9); for a 100-emitter array up to 5.4 W has been achieved (1) (Fig. 2). These very high cw power levels are now in a realm that until recently could only be achieved with large, and much less efficient, laser systems such as argon ion and neodymium-doped yttrium aluminum garnet (Nd:YAG).

At the ultimate power levels reached by the lasers in Fig. 2, the devices fail almost instantly in a research laboratory environment because of the catastrophic mirror failure mechanism described above. To obtain a reasonably long useful lifetime (thousands of hours), it is necessary to operate the devices at a power level that does not exceed 20 to 30% of the catastrophic mirror damage limit. Thus, for example, although the best single-emitter laser can produce more than 200 mW, the best commercially available single-

emitter devices are rated at no more than 50 mW. Similar derating must be applied to multi-emitter arrays as well, and the highest power 10-emitter array that is commercially available (10) is rated at 500 mW cw.

Ultrahigh-Power Quasi-cw Laser Diode Arrays

From the preceding discussion, it can be seen that the advent of the multi-emitter array configuration has increased the continuous power available from semiconductor lasers from milliwatts to watts. By further extending the number of emitters, outputs in the kilowatt range have been achieved during long pulses. In Fig. 2 it can be observed that the available output power does not increase linearly with the number of emitters in the array. This occurs because it becomes progressively more difficult to remove waste heat as the size of the array increases. As a result, the 100-emitter array can only deliver about four times the power of the 10-emitter array. For more than 100 emitters the thermal problem is exacerbated, and the peak cw power can no longer be increased by adding emitters. If the arrays are operated in long pulses (hundreds of microseconds) with a low duty factor (a few percent), however, the peak power can be increased by several orders of magnitude. This mode of operation is referred to as quasi-cw because the chip reaches its local equilibrium temperature in a few microseconds, but the rate of power dissipation precludes continuous operation. Because of their high efficiency and reliability, quasi-cw arrays are now being intensively developed as pump sources for pulsed solid-state lasers such as Nd:YAG.

An exploded schematic diagram of a two-dimensional ultrahigh-power quasi-cw array is shown in Fig. 3. An extended "bar," up to 1 cm long and containing up to 1000 individual emitters, is soldered active side down at the front edge of a mounting plate made of material with high thermal conductivity, such as BeO in Fig. 3 (11). The BeO plate is metallized in a pattern such that the entire linear array can be driven in parallel by applying a voltage between the top and bottom surfaces of the plate.

The light-versus-current characteristics of a high-quality, 1-cm-wide linear array of emitters are shown in Fig. 4A. The quasi-cw (150- μ sec pulses) optical output reaches 100 W at a drive current of about 90 A. This device has a very high (>80%) differential efficiency above threshold that leads to an overall power conversion efficiency of about 50%. Power conversion efficiencies as high as 57% have been obtained from less powerful laser diodes, which is the highest efficiency reported for a laser of any kind (12). For comparison, the efficiency of lamp-pumped solid-state lasers is no higher than 1 to 5%, and for ion lasers the efficiency is well below 0.1%.

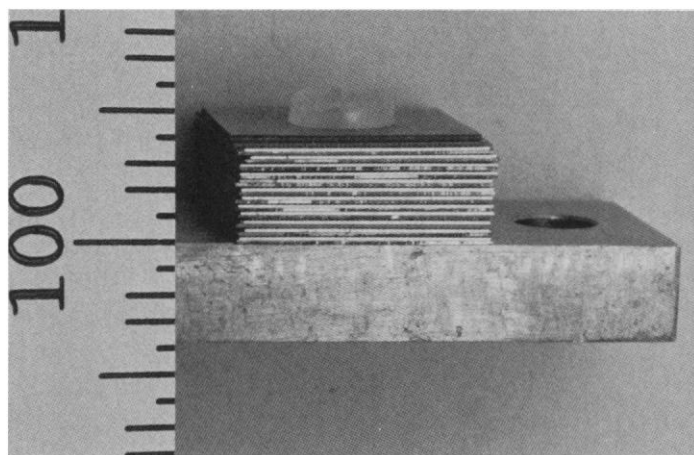


Fig. 5. Photograph of a two-dimensional array of 12,000 emitters. The white horizontal lines are the facets of the individual bars, and the regions between are the edges of the thin mounting plates. The scale at the left is in millimeters.

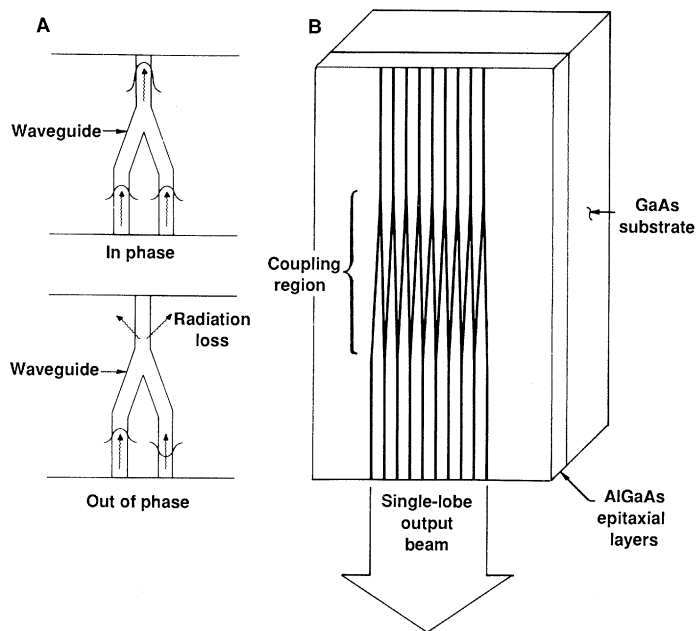


Fig. 6. (A) Principle of operation of a waveguide Y-junction. (B) A schematic diagram of an array of Y-coupled diode laser emitters.

Because the linear arrays are mounted on thin plates, they can be stacked into high-density two-dimensional configurations as shown in Fig. 3. A completely characterized linear subassembly that has passed rigid production testing is placed on a bottom mounting plate and held in position by precision alignment pins. Next, a thin metallic spacer is placed on the linear array subassembly to provide mechanical clearance and to conduct current from the next stack level. This process is repeated until the desired stack size (output power capability) is reached. The entire two-dimensional array is driven by a single power source connected only to the top and bottom mounting plates. With current technology, linear array subassemblies can be stacked to a density of about 30 per centimeter, and optical power densities well in excess of 3 kW/cm² have been achieved.

A prototype two-dimensional array of diode lasers is shown in Fig. 5 (3). This device consists of 12 linear arrays stacked to create an effective emitting area of 4 mm by 10 mm, and there are approximately 12,000 individual diode lasers contained within the active aperture. An example of the results achieved from such a stack

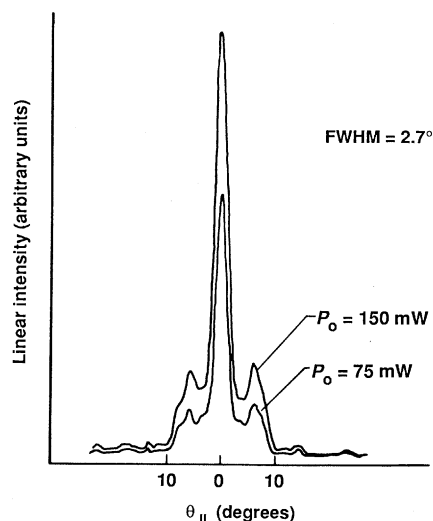


Fig. 7. Plot of the output beam profile of a Y-junction array of diode lasers at two different power levels exhibiting a high degree of collimation. FWHM, full width at half-maximum; P_o , output power; $\theta_{||}$, deviation from facet normal.

of 12 linear arrays is shown in Fig. 4B. The threshold current for the stack (17 A) is about the same as that for a single linear. More than 600 W of quasi-cw power was achieved, which corresponds to more than 1.5 kW/cm², well below the catastrophic damage limit. The power conversion efficiency for the entire stack was 38%.

Progress in Coherent High-Power Arrays

The cw and quasi-cw arrays described above have the desirable attributes of high power, high efficiency, small size, narrow emission bandwidth, and high reliability. The laser output beam pattern, however, is not coherent because the relative phasing of the large number of individual emitters is difficult to control. Recently, substantial improvements in the beam quality obtained from multi-emitter arrays have been achieved by a number of methods, one of which makes use of internal waveguide Y-junctions (13-15). The principle of operation of Y-junctions is shown in Fig. 6. The objective is to force all emitters to be in phase with one another. If the waves in the two input legs of the Y-junction are in phase, they will constructively interfere and combine with little loss in the output waveguide. If the waves are 180° out of phase, they will destructively interfere and radiate out of the waveguides. Thus, in an array of Y-junctions, the mode of oscillation in which all waveguides are in phase will experience the least loss at the junctions and will therefore be the preferred mode.

Figure 7 shows the far-field patterns for a Y-junction array of nine emitters on 6- μ m centers at two different cw power levels. The light is contained predominantly in a narrow central lobe that is stable with respect to variation in power level. The width of the pattern is within a factor of 2 of the diffraction limit calculated for the total emitting aperture, indicating excellent phase locking among the individual emitters. (The small, residual side lobes result from the periodic nature of the array and are similar in origin to higher orders of diffraction from a grating.) Thus, these mode-controlled arrays offer the potential of achieving both high power and the beam quality necessary for many applications that until now required very large ion or solid-state laser systems.

Conclusions

The rapid progress being achieved in diode laser arrays can be summarized by plotting the commercially available power level (that

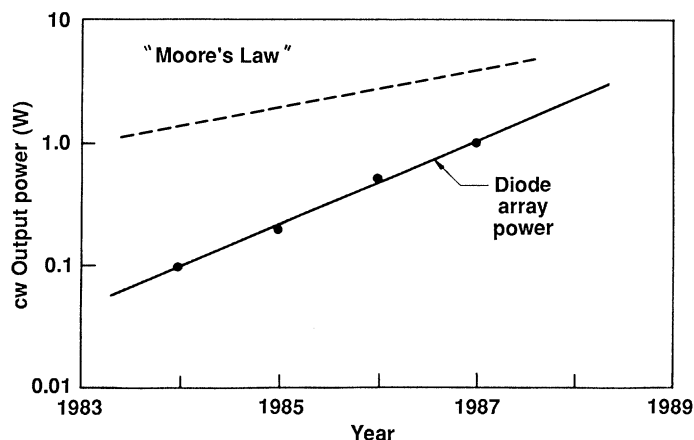


Fig. 8. A plot of the output power available commercially from multi-emitter diode laser arrays as a function of calendar year. Shown for comparison is "Moore's Law" for the density of electronic devices on a single silicon chip.

is, the rating for long useful lifetime) versus calendar years (Fig. 8). The first 10-emitter arrays appeared in 1984 and were rated at 100 mW. Since that time, the reliable power level has approximately doubled every year, and 1-W devices are available today (16). It is likely that this rapid progression can be sustained for at least several more years.

The dashed line in Fig. 8 depicts "Moore's Law" for silicon integrated circuits. In the early 1970s, Gordon Moore, one of the founders of Intel Corporation, observed that the number of components that could be integrated onto a single silicon chip was doubling every 2 years. For comparison, the output power available from diode lasers is increasing at a rate twice as great. Thus substantial technological spin-off from these rapidly developing optical "integrated circuits" is certain to follow in the near future.

REFERENCES AND NOTES

1. G. L. Harnagel, D. R. Scifres, H. H. Kung, D. F. Welch, P. S. Cross, *Electron. Lett.* **22**, 605 (1986).
2. G. L. Harnagel, P. S. Cross, C. R. Lennon, M. DeVito, D. R. Scifres, *ibid.* **23**, 743 (1987).
3. G. L. Harnagel, P. S. Cross, C. R. Lennon, D. R. Scifres, in preparation.
4. D. R. Scifres, C. Lindstrom, R. D. Burnham, W. Streifer, T. L. Paoli, *Electron. Lett.* **19**, 169 (1983).
5. N. Holonyak, R. M. Kolbas, R. D. Dupuis, P. D. Dapkus, *IEEE J. Quantum Electron.* **QE-16**, 170 (1980).
6. R. D. Burnham, W. Streifer, D. R. Scifres, C. Lindstrom, T. L. Paoli, *Electron. Lett.* **18**, 1095 (1982).
7. K. Hamada *et al.*, *IEEE J. Quantum Electron.* **QE-21**, 623 (1985).
8. C. H. Henry, P. M. Petroff, R. A. Logan, F. R. Merritt, *J. Appl. Phys.* **50**, 3721 (1979).
9. D. F. Welch *et al.*, *Electron. Lett.* **22**, 464 (1986).
10. Model SDL-2430 from Spectra Diode Laboratories, San Jose, CA.
11. G. L. Harnagel *et al.*, *Appl. Phys. Lett.* **49**, 1418 (1986).
12. D. S. Hill *et al.*, in *Digest of the Topical Meeting on Semiconductor Lasers* (paper WB-8), Albuquerque, NM, 10 and 11 February 1987.
13. K. L. Chen and S. Wang, *Electron. Lett.* **22**, 644 (1986).
14. D. F. Welch, P. S. Cross, D. R. Scifres, W. Streifer, R. D. Burnham, *Appl. Phys. Lett.* **49**, 1632 (1986).
15. W. Streifer, P. S. Cross, D. F. Welch, D. R. Scifres, *ibid.*, p. 58.
16. Model SDL-2460 from Spectra Diode Laboratories, San Jose, CA.
17. We thank D. P. Worland, C. Lennon, and H. H. Kung for many useful technical discussions and the Defense Advanced Research Projects Agency and the Naval Ocean Systems Center for support of the two-dimensional array work.

Activated Oncogenes in B6C3F1 Mouse Liver Tumors: Implications for Risk Assessment

STEVEN H. REYNOLDS,* SHARI J. STOWERS, RACHEL M. PATTERSON,
ROBERT R. MARONPOT, STUART A. AARONSON, MARSHALL W. ANDERSON

The validity of mouse liver tumor end points in assessing the potential hazards of chemical exposure to humans is a controversial but important issue, since liver neoplasia in mice is the most frequent tumor target tissue end point in 2-year carcinogenicity studies. The ability to distinguish between promotion of background tumors versus a genotoxic mechanism of tumor initiation by chemical treatment would aid in the interpretation of rodent carcinogenesis data. Activated oncogenes in chemically induced and spontaneously occurring mouse liver tumors were examined and compared as one approach to determine the mechanism by which chemical treatment caused an increased incidence of mouse liver tumors. Data suggest that furan and furfural caused an increased incidence in mouse liver tumors at least in part by induction of novel weakly activating point mutations in *ras* genes even though both chemicals did not induce mutations in *Salmonella* assays. In addition to *ras* oncogenes, two activated *raf* genes and four non-*ras* transforming genes were detected. The B6C3F1 mouse liver may thus provide a sensitive assay system to detect various classes of proto-oncogenes that are susceptible to activation by carcinogenic insult. As illustrated with mouse liver tumors, analysis of activated oncogenes in spontaneously occurring and chemically induced rodent tumors will provide information at a molecular level to aid in the use of rodent carcinogenesis data for risk assessment.

SEVERAL APPROACHES HAVE BEEN USED TO IDENTIFY ENVIRONMENTAL agents that pose significant carcinogenic hazards to humans. Chemicals in the environment are assessed on the basis of epidemiologic evidence from exposed human populations, when available, with supportive evidence derived from short-term tests that correlate with carcinogenicity. However, most chemicals are classified as potentially hazardous to humans on the basis of long-term carcinogenesis studies in rodents. Although animal experiments are designed so as to mimic the route of human exposure in the environment or workplace, the doses used in animals are usually higher than those to which humans are actually exposed. High doses of a chemical are utilized to enhance the sensitivity of the assay, since economic considerations limit the number of animals that can be used per study. The extrapolation of rodent carcinogenic data to human risk is complicated by the higher doses used in animals, and especially by the absence of information regarding the mechanisms of tumor induction.

Short-term tests have been utilized to evaluate the potential hazards of chemicals to humans. These tests have been popular because they can be performed quickly and inexpensively relative to long-term rodent carcinogenesis assays. Initially, many of the chemi-

S. H. Reynolds, S. J. Stowers, R. M. Patterson, M. W. Anderson, Laboratory of Biochemical Risk Analysis, National Institute of Environmental Health Sciences, Post Office Box 12233, Research Triangle Park, NC 27709. R. R. Maronpot, National Toxicology Program, National Institute of Environmental Health Sciences, Post Office Box 12233, Research Triangle Park, NC 27709. S. A. Aaronson, Laboratory of Cellular and Molecular Biology, National Institutes of Health, Bethesda, MD 20205.

*To whom reprint requests should be addressed.